Analyst

PAPER

View Article Online
View Journal | View Issue



Cite this: *Analyst*, 2015, **140**, 1543

# Electroanalytical detection of pindolol: comparison of unmodified and reduced graphene oxide modified screen-printed graphite electrodes†

Loanda R. Cumba,[a,b] Jamie P. Smith,[a] Dale A. C. Brownson,[a] Jesús Iniesta,[c] Jonathan P. Metters,[a] Devaney R. do Carmo[b] and Craig E. Banks*[a]

Received 1st November 2014,
Accepted 9th January 2015

DOI: 10.1039/c4an02005g

www.rsc.org/analyst

Recent work has reported the first electroanalytical detection of pindolol using reduced graphene oxide (RGO) modified glassy carbon electrodes [S. Smarzewska and W. Ciesielski, *Anal. Methods*, 2014, **6**, 5038] where it was reported that the use of RGO provided significant improvements in the electroanalytical signal in comparison to a bare (unmodified) glassy carbon electrode. We demonstrate, for the first time, that the electroanalytical quantification of pindolol is actually possible using bare (unmodified) screen-printed graphite electrodes (SPEs). This paper addresses the electroanalytical determination of pindolol utilising RGO modified SPEs. Surprisingly, it is found that bare (unmodified) SPEs provide superior electrochemical signatures over that of RGO modified SPEs. Consequently the electroanalytical sensing of pindolol is explored at bare unmodified SPEs where a linear range between 0.1 μM–10.0 μM is found to be possible whilst offering a limit of detection (3σ) corresponding to 0.097 μM. This provides a convenient yet analytically sensitive method for sensing pindolol. The optimised electroanalytical protocol using the unmodified SPEs, which requires no pre-treatment (electrode polishing) or electrode modification step (such as with the use of RGO), was then further applied to the determination of pindolol in urine samples. This work demonstrates that the use of RGO modified SPEs have no significant benefits when compared to the bare (unmodified) alternative and that the RGO free electrode surface can provide electro-analytically useful performances.

## Introduction

Pindolol [1-(indol-4-yioxy)-3-isopropylaminopropan-2-ol] is a β-adrenergic blocking substance widely used for the treatment of hypertension, angina and glaucoma.[1] Its molecular structure (see Scheme 1) has an indole group to which a chain of isopropylaminopropoxy is connected; this side chain is characteristic of β-blockers such as pindolol and the aromatic fragment induces specific pharmacokinetic properties.[2] Pindolol is administrated as a racemic mixture and of the two enantiomers, the *S* (−)-pindolol is considerably more potent than the *R* (+)-pindolol as a β-blocker.[3–5]

Pindolol is also a drug which is widely used to combat hypertension in pregnancy, causing no harm to the fetus whilst significantly improving the renal functions of pregnant women.[6] The drug has currently been highlighted in the field of antidepressants because the co-administration of pindolol with selective serotonin reuptake inhibitors (SSRIs) has been reported to enhance the increase of 5-HT transmission in cortical and limbic[7] areas, in turn resulting in the symptomatic relief of depression. However, pindolol has lipophilic properties and is practically insoluble in water at basic pH.[1,8]

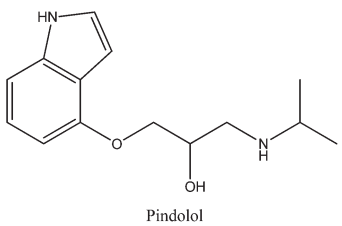


Pindolol

**Scheme 1** Molecular structure of pindolol.

[a]*Faculty of Science and Engineering, School of Chemistry and the Environment, Division of Chemistry and Environmental Science, Manchester Metropolitan University, Chester Street, Manchester M1 5GD, UK. E-mail: c.banks@mmu.ac.uk; http://www.craigbanksresearch.com; Fax: +44 (0)161-247-6831; Tel: +44 (0)161-247-1196*

[b]*Faculdade de Engenharia de Ilha Solteira UNESP – Universidade Estadual Paulista, Departamento de Física e Química, Av. Brasil Centro, 56 CEP 15385-000, Ilha Solteira, SP, Brazil*

[c]*Physical Chemistry Department and Institute of Electrochemistry, University of Alicante, 03690 San Vicente del Raspeig, Alicante, Spain*

†Electronic supplementary information (ESI) available. See DOI: 10.1039/c4an02005g

When administered in high doses it can mistakenly cause bronchodilation and tachycardia.[9]

Analytical techniques reported within the literature for the determination of pindolol include spectrofluorimetry,[10] liquid chromatography-tandem mass spectrometry[11] and high-performance liquid chromatography.[12–14] Notably however, only one report for the electrochemical determination of pindolol exists within the literature;[15] which is a potentially rapid, facile and low cost protocol for the monitoring of such a key analyte.

In the first (and only) report concerning the electrochemical detection of pindolol, Smarzewska and Ciesielski,[15] stated that reduced graphene oxide (RGO) modified glassy carbon (GC) electrodes exhibit significantly increased peak currents towards the electrochemical oxidation of pindolol in comparison to bare (unmodified) GC electrodes.[15] The approach, whilst noteworthy, requires a GC electrode to be polished and diligently modified with RGO prior to electrochemical measurements being performed, thus resulting in a potentially inefficient (speed), unreliable (repeatability) and erroneous procedure. We also note that the paper lacks sufficient morphological characterization of the RGO used, including analysis of the RGO after its deposition onto the supporting electrode surface.

When considering electrochemical sensing protocols, one electrochemical configuration which boasts a plethora of advantages as a sensing platform are screen-printed graphite electrodes (SPEs). These useful electrode configurations have attracted considerable attention in recent years due to efficiency, speed and low cost, as well as being portable, disposable and requiring no surface pretreatment or polishing.[16–24] Much interest in the development of new and novel screen-printed electrode configurations prevail owing to the portability of the technology, something that arouses interest worldwide since the use of such electrodes allow analysis "in the field".

In this paper we demonstrate, for the first time, that pindolol can be electrochemically quantified using SPEs at analytically relevant concentrations in both 'ideal' laboratory conditions and in urine samples. Furthermore, we critically compare the response of unmodified SPEs with that of RGO modified SPEs, questioning the use of the latter over that of the former.

## Experimental

All chemicals were of the highest grade available and were used as received (without further purification) from Sigma Aldrich (UK). All solutions were prepared using deionised water of resistivity no less than 18.2 MΩ cm and were vigorously degassed prior to electrochemical measurements with high purity, oxygen free nitrogen. Solutions containing 1.0 mM of pindolol in 0.1 M of potassium chloride (KCl) were used on the day of preparation. Working solutions of lower concentrations were prepared by appropriate dilution of the stock solution as mentioned above. Solutions with different pH values were prepared in order to further studies.

Voltammetric measurements were carried out using a μ-AutolabIII (Eco Chemie, The Netherlands) potentiostat/galvanostat and controlled by Autolab GPES (General Purpose Electrochemical System) software version 4.9. All electrochemical measurements were performed at room temperature. A conventional three-electrode system was used where screen-printed graphite electrode (working electrode) with on-board graphite counter and Ag/AgCl reference electrodes. All potentials are referred to utilizing this reference electrode. All electrochemical experiments were performed at room temperature. Square wave parameters (frequency and amplitude) were optimised prior to experimentation.

Scanning electron microscope (SEM) images and surface element analysis were obtained with a JEOL JSM-5600LV model equipped with an energy-dispersive X-ray (EDX) microanalysis package. Raman Spectroscopy was performed using a Renishaw InVia spectrometer with a confocal microscope (×50 objective) spectrometer with an argon laser (514.3 nm excitation) at a very low laser power level (0.8 mW) to avoid any heating effects. X-ray Photoelectron Spectroscopy (XPS) measurements were performed with a Kratos Axis Ultra spectrometer using monochromatic Al K X-rays (1486.6 eV) (performed independently by CERAM40).

### Fabrication of screen-printed graphite sensors (SPEs)

The screen-printed graphite electrodes (SPEs) utilized consist of a graphite working electrode, a graphite counter electrode and a Ag/AgCl reference electrode. The screen-printed graphite electrodes, which have a 3 mm diameter working electrode, were fabricated in-house with appropriate stencil designs using a microDEK 1760RS screen-printing machine (DEK, Weymouth, UK). This screen-printed electrode design has been previously reported.[19,24–26] For the case of each fabricated electrode, first a graphite ink formulation (Product Code: C2000802P2; Gwent Electronic Materials Ltd, UK), which is utilized for the efficient connection of all three electrodes and as the electrode material for both the working and counter electrodes, was screen-printed onto a polyester (Autostat, 250 micron thickness) flexible film. After curing the screen-printed graphite layer in a fan oven at 60 degrees Celsius for 30 minutes, next a Ag/AgCl reference electrode was included by screen-printing Ag/AgCl paste (Product Code: C2040308D2; Gwent Electronic Materials Ltd, UK) onto the polyester substrates, which was subsequently cured once more in a fan oven at 60 degrees for 30 minutes. Finally, a dielectric paste (Product Code: D2070423D5; Gwent Electronic Materials Ltd, UK) was then screen-printed onto the polyester substrate to cover the connections and define the active electrode areas, including that of the working electrode (3 mm diameter). After curing at 60 degrees for 30 minutes the SPEs are ready to be used. These electrodes have been characterized electrochemically in a prior paper[19] and have heterogeneous electron transfer rate constants of $1.08 \times 10^{-3}$ cm $s^{-1}$ using 1 mM hexaammine-ruthenium(III) chloride/0.1 M KCl. The reproduci-

 

bility and repeatability of the fabricated batches of electrodes were explored through comparison of cyclic voltammetric responses using 1 mM hexaammine-ruthenium(III) chloride/0.1 M KCl. Analysis of the voltammetric data revealed the % relative standard deviation (%RSD) to correspond to no greater than 0.82% ($N$ = 20) and 0.76% ($N$ = 3) for the reproducibility and repeatability of the fabricated SPEs (for use in electroanalysis).

### Modification of screen-printed graphite electrodes with reduced graphene oxide (RGO)

A solution containing 2.0 mg of 'high surface area reduced graphene oxide' (denoted as RGO) (Graphene Supermarket, USA) in 0.5 mL of methanol was prepared. The manufacturing method for 'high surface area' RGO is the Thermal Reduction of graphene oxide, which in turn is produced from graphite by the Hummer's Method. The exact details of the method are proprietary information and as such not readily available from the supplier. A homogeneous and stable suspension was obtained through the use of an ultrasonic bath (10 minutes). The screen-printed graphite electrodes were modified by drop-casting using different aliquots with a micropipette. After 30 minutes the methanol was evaporated (at ambient temperature) and the modified electrodes were then ready for use.

Independent characterisation of the RGO was performed using SEM, Raman and XPS analysis. Fig. 1A shows the SEM micrograph of RGO on a $SiO_2$ plate whilst in Fig. 1B the RGO can be observed once modified upon a SPE. The characteristic flake-like-crumpled structure of RGO is evident in both SEM micrographs, with the apparent presence of both single and few-layered regions of RGO forming after solvent (carrier) evaporation due to natural coalescence, where additionally it is clear that the RGO becomes integrated with the supporting electrode surface in Fig. 1B.[27] Fig. 2 depicts Raman spectra of the commercially sourced RGO, which shows two distinct characteristics depending on where the RGO sample was probed. The Raman spectrum shown in Fig. 2A reveals two characteristic peaks at *ca.* 1580 and 2690 $cm^{-1}$ that are due to the G and 2D (G′) bands of graphitic structures respectively.[28–30] The highly symmetrical 2D (G′) peak indicates that the material is comprised of few-layer graphene (consistent with SEM images). Additionally, the intensity ratio of the G and 2D bands (G/2D = 1.50) indicates that the graphene sheets are indeed stacked and comprised of few-layer graphene domains, where the high intensity of the G band in relation to the 2D peak is characteristic of multi-layered graphene (but in this case does not display the characteristics of graphite).[28–30] The presence of a D band at *ca.* 1350 $cm^{-1}$ indicates a that the RGO has a number of structural defects on across its surface (limited basal plane crystal defects), which is as expected given the fabrication method.[31] In contrast, although the Raman spectrum shown in Fig. 2B reveals a characteristic peak at

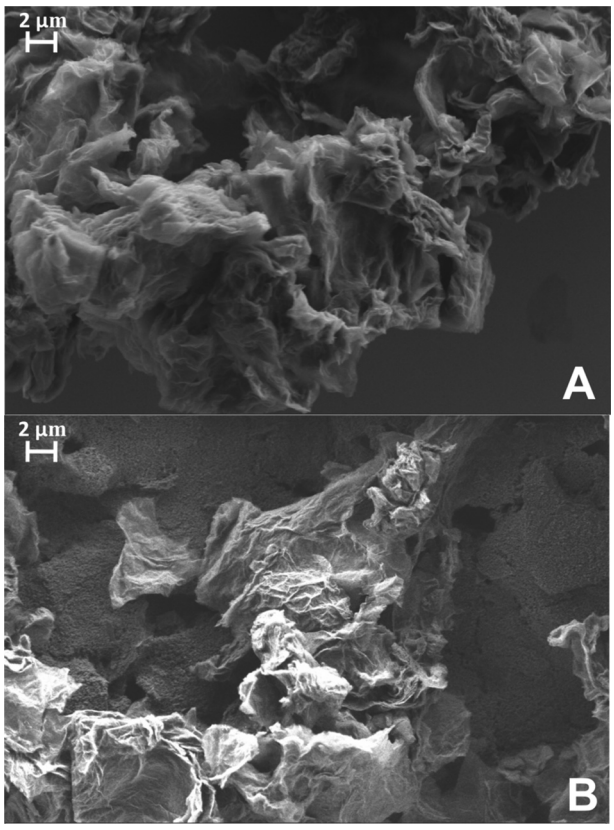


**Fig. 1** SEM images of (A) 2.0 μg of RGO immobilized upon a $SiO_2$ plate and (B) 2.0 μg of RGO immobilized upon a SPE.

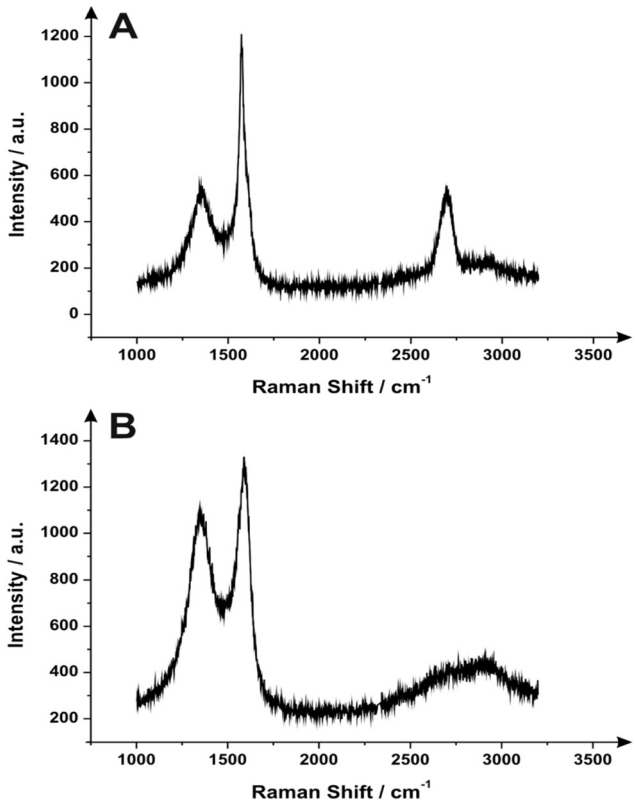


**Fig. 2** Raman spectra of the commercially obtained RGO. Spectra were recorded from various areas across the sample, the two shown are representative.

*ca.* 1580 $cm^{-1}$ which is due to the G band of graphitic structures, at *ca.* 2840 $cm^{-1}$ a wave-like protrusion is evident from the baseline which is characteristic of graphene oxide.[32,33] In this case, the presence of a D band at *ca.* 1350 $cm^{-1}$ (which is of an intensity similar to the adjacent G band) is a further indication that graphene oxide is present (with a large number of structural defects on/across its surface (limited basal plane crystal defects due to the oxygenated material)).[32,33] Given insights obtained from the SEM and Raman analysis presented above, it is clear that the commercially sourced RGO used herein consists of regions of both few-layer graphene and graphene oxide and thus is actually *partially reduced graphene oxide*, which is as expected and widely reported in the literature.[32,33] The XPS spectrum shown in ESI Fig. 1† confirms the above inferences and thus the presence of partially reduced graphene oxide as determined through comparison to reports in the literature.[27,34–36] ESI Table 1† lists the surface atomic composition of RGO in atomic percentage (at%), the total atomic percentage for carbon (C%) is 91.87 and for oxygen (O%) is 8.13.

### Analysis of urine samples

The urine analyzed was collected from healthy donors in the morning, free of interfering drugs. Solutions of urine containing pindolol were prepared as follows: 0.1 μM (sample 1); 1.0 μM (sample 2) and 10.0 μM (sample 3). Urine samples were modified to facilitate electrochemical measurements with samples containing 0.1 M KCl. All urine samples were prepared and analyzed on the day of collection.

## Results and discussion

First, cyclic voltammetric measurements using screen-printed graphite electrodes (SPEs) were conducted over a range of pH (2–9) as depicted in Fig. 3, where one can observe a well-defined voltammetric signal ~+0.89 V (*vs.* Ag/AgCl). From inspection of Fig. 3, one can clearly see that the peak potential of the electrochemical signal does not move with pH, indicating that the electrochemical mechanism does not involve the transfer of protons; the sole presence of an oxidation peak suggests that this is an electrochemically irreversible reaction.[37] Given the pH independence of the voltammetric response, the electrochemical mechanism likely involves the electrochemical oxidation of the secondary amine present on pindolol producing oxipindolol. Also observed is an increase in the intensity of the anodic peak current with an increased concentration of hydrogen ions in solution, *i.e.* acidic solutions favor the solubility of pindolol thus facilitating the electrochemical oxidation and increased voltammetric peak magnitude for pindolol (*viz.* Fig. 3A). Pindolol is lipophilic and is largely insoluble at alkaline pHs;[8,38] since the solubility is highly dependent on the hydrogen ion concentration;[38] this information is valuable for the optimization of the electroanalytical system. Based on the above results, where pH 2 gives the largest electrochemical signal, this pH was used herein.

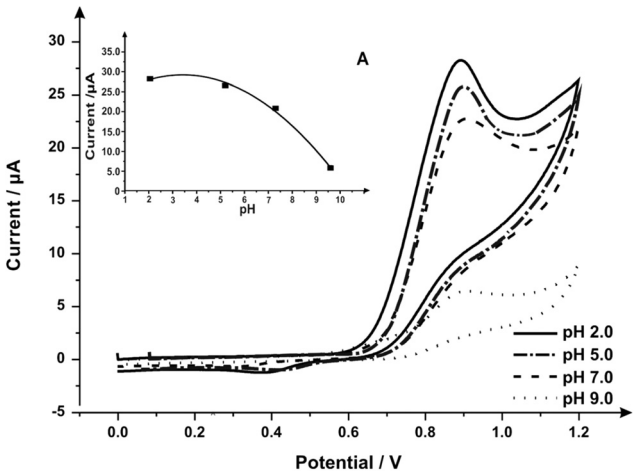


**Fig. 3** Cyclic voltammetric study exploring the variation of pH obtained in a solution containing 1 mM pindolol/0.1 KCl using SPEs. Part (A) a plot of current as a function of pH variation of pindolol. Scan rate: 100 mV $s^{-1}$ *vs.* Ag/AgCl.

To further explore the electrochemical response of pindolol, different electrode substrates were tested towards its electrochemical oxidation to allow for comparison with the response obtained using the SPEs. Fig. 4 depicts the voltammetric responses of the screen-printed graphite, boron doped diamond (BDD), glassy carbon (GC) and edge-plane pyrolytic graphite (EPPG) electrodes. These electrodes show clear and well defined voltammetric peaks, which are observed at +0.89 V (*vs.* Ag/AgCl) using a SPE, +0.88 V (*vs.* Ag/AgCl) for BDD, +0.95 V (*vs.* Ag/AgCl) for GC and +0.84 V (*vs.* Ag/AgCl) for EPPG. Analysis of the responses obtained using the explored electrode materials revealed the EPPG electrode to exhibit the highest current density (508.9 μA $cm^{-2}$), whilst the BDD (397.9 μA $cm^{-2}$), SPE (398.2 μA $cm^{-2}$) and GC (383.9 μA $cm^{-2}$) electrodes all reveal similar electrochemical performances with

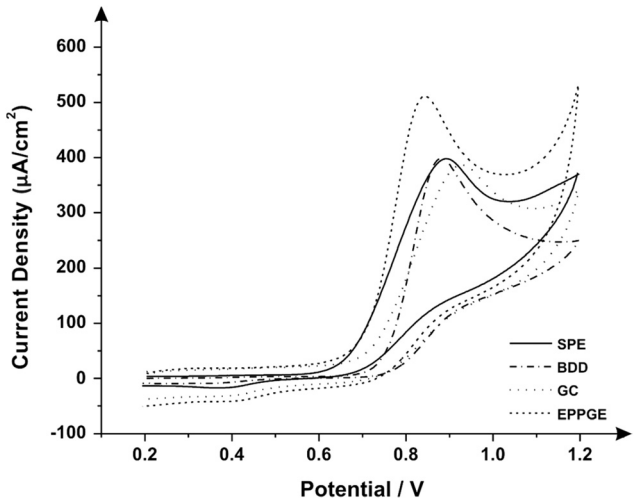


**Fig. 4** Cyclic voltammograms obtained in 1 mM pindolol/0.1 KCl (pH: 2, scan rate: 100 mV $s^{-1}$, *vs.* Ag/AgCl) utilising the following electrodes: SPE, BDD, GC and EPPG.

regard to current density (densities were calculated using the geometric area of the electrode surfaces). The effect of scan rate for each electrode substrate was explored where a plot of voltammetric peak height against the square-root of scan rate was constructed: EPPG: $I_p/A = 2.048 \times 10^{-4}$ A $(V\ s^{-1})^{-0.5} + 1.750 \times 10^{-5}$ A; $R^2 = 0.948$, SPE: $I_p/A = 6.657 \times 10^{-5}$ A $(V\ s^{-1})^{-0.5} + 5.246 \times 10^{-6}$ A; $R^2 = 0.993$, BDD: $I_p/A = 7.557 \times 10^{-5}$ A $(V\ s^{-1})^{-0.5} + 2.156 \times 10^{-6}$ A; $R^2 = 0.985$, GC: $I_p/A = 5.462 \times 10^{-5}$ A $(V\ s^{-1})^{-0.5} + 7.515 \times 10^{-6}$ A; $R^2 = 0.936$. In all instances there was a linear correlation which is indicative that the electrochemical oxidation of pindolol is governed by a diffusional process (as opposed, to say, an adsorbed process). Considering the electrochemical performance of the electrode materials (*viz.* Fig. 4) it can be concluded that although the EPPG electrode attained the greatest voltammetric signal in terms of the analytically important current density, the alleviation for the requirement of polishing offered by SPEs is of significant value, particularly given that the voltammetric signal obtained using the screen-printed sensor was comparable to that of the EPPG electrode. Consequently, work herein focuses upon the use of the SPEs.

In attempts to further enhance the electroanalytical potential of the SPE configuration, modification of the graphite working electrode surface through the deposition of reduced graphene oxide (RGO) was next considered. RGO is an innovative material used to modify electrodes and it is widely reported to improve the electrochemical response in such cases.[39–42] Furthermore, recent reports have suggested that the modification of carbon-based electrode substrates with RGO can yield an improved electroanalytical determination of pindolol[15] utilizing square-wave voltammetry. Consequently, RGO was next used to explore the potential electrochemical improvements towards pindolol determination over unmodified (bare) SPEs as reported within the literature.[15] The SPEs were modified as described in the Experimental section. Fig. 5 depicts the square wave voltammetric responses obtained in a 1.0 mM pindolol/0.1 M KCl solution using RGO modified SPEs, which are critically compared to that of a bare SPE. Fig. 5 depicts the analysis of the voltammetric peak potential (inserts in Fig. 5) and peak height as a result of increasing amounts (masses) of RGO where it can readily be observed that the initial voltammetric results become deteriorated with the voltammetric peak shifting to higher potentials and the peak current decreasing in magnitude. Comparison of a bare (unmodified) SPE with that of modified RGO SPEs reveals the response of the former to be optimal over that of the latter due to the largest voltammetric peak heights (analytical signal) and less facile potential being obtained; one then questions the need to use RGO at all. The origin of this poor response might be due to poor electrical wiring of the RGO upon the electrode surface or a repulsive interaction between reduced graphene oxide and pindolol.

Fig. 6 shows a Raman map of a RGO modified SPE, confirming uniform coverage of the electrode, indicating the responses observed in Fig. 6 can be attributed to the RGO and not the underlying electrode substrate or a combination of

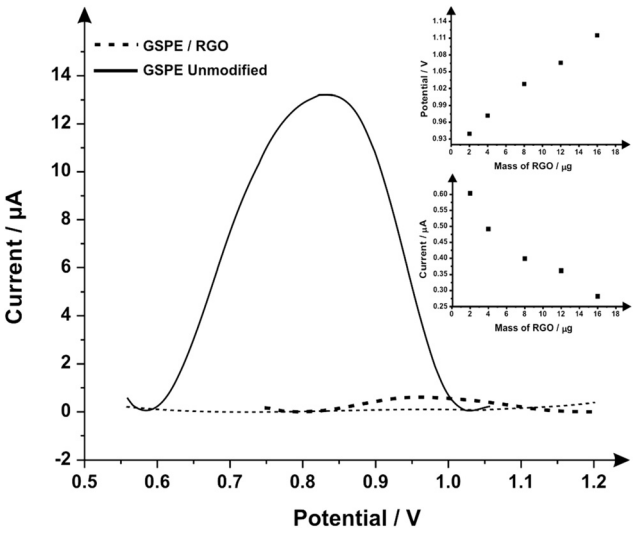


**Fig. 5** Comparison of a bare/unmodified SPE (solid line) with that of a RGO (2.0 µg) modified SPE (dashed line) using square wave voltammetry recorded in a solution comprising 1 mM pindolol/0.1 M KCl. Square-wave parameters: step potential = 0.00705 V, frequency = 50 Hz, amplitude = 50 mV, deposition potential = 0.5 V with duration = 10 s *vs.* Ag/AgCl. Also shown is the response of a bare/unmodified SPE in the absence of pindolol (dotted line). Shown in the inserts are the responses of the peak potential and current as a function of increasing amounts (mass) of RGO.

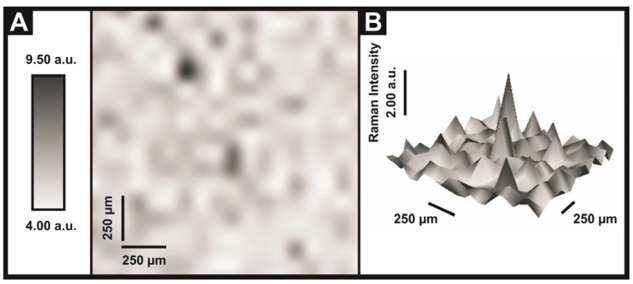


**Fig. 6** Raman maps of a central area on the SPEs following modification with 2.0 µg RGO. Raman intensities are recorded at *ca.* 1580 $cm^{-1}$.

both. Through analysis of Fig. 5 it is clear that the modification of SPEs with RGO is not advantageous when compared directly to the performance of the unmodified (bare) alternative since the modified electrodes exhibit the electrochemical oxidation of pindolol at much higher (positive) potential regions whilst possessing weaker analytical signals (peak currents). Furthermore, the lengthy preparation of the electrode modification process in order to yield such negative results means that one can discard this type of electrode modification for further studies towards the electroanalytical oxidation of pindolol.

Having determined that the modification of the SPEs surface with RGO offered no significant or viable improvement in the electrochemical sensor with regard to pindolol determination, the electroanalytical performance of the unmodified screen-printed graphite electrode was next explored. Additions of pindolol were made over the concentration range

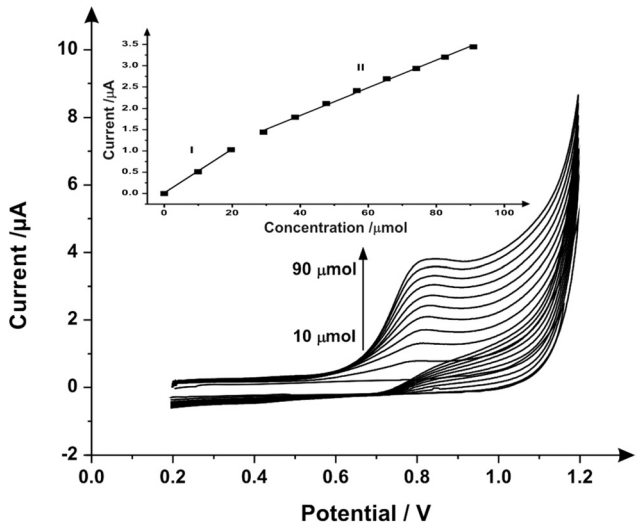


Fig. 7 Cyclic voltammograms resulting from increasing additions of pindolol concentrations (10–90 µM) using a bare/unmodified SPE (scan rate: 100 mV $s^{-1}$ *vs.* Ag/AgCl) into a pH buffer solution; the dotted line represents a blank. Inset: analysis of the voltammetric profiles in terms of the peak height as a function of concentration where two analytical curves are evident, corresponding to the anodic peak current for the oxidation of pindolol over the concentration range.

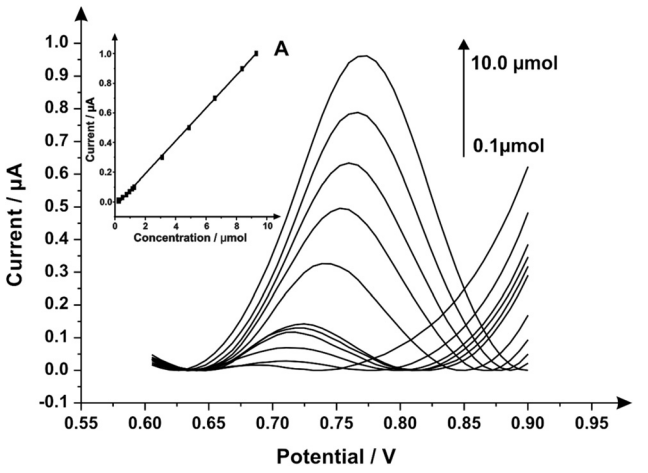


Fig. 8 Square wave voltammograms recorded over a range of pindolol concentrations (0.1–10.0 µM) in 0.1 M KCl at pH 2.0 (step potential = 0.00705 V, frequency = 50 Hz, amplitude = 50 mV, deposition potential = 0.5 V and duration = 10 s *vs.* Ag/AgCl) using a bare/unmodified SPE; the dotted line represents a blank. (A, inset) An analytical curve corresponding to the anodic peak for the oxidation of pindolol over the concentration range.

of 10 µM–90 µM into a pH 2 buffer solution. Fig. 7 depicts the voltammetric signatures where analysis of the voltammetric peak height (current) reveals two linear responses (see inset of Fig. 7). The first is over the range 10 µM–20 µM, ($I_P$/µA = 0.0526 A L $mol^{-1}$ + 0.0029 µA; $R^2$ = 0.9999 and $N$ = 3) and the second from 30 µM to 90 µM, ($I_P$/µA = 0.0321 A L $mol^{-1}$ + 0.5614 µA; $R^2$ = 0.9978 and $N$ = 3); based on the first linear range a limit of detection (3σ) of 0.38 µM is possible and a percentage relative standard deviation (%RSD) of 5.74% resulting from the analysis of the voltammetric peak height.

The square wave voltammograms obtained utilizing the SPEs through the additions of pindolol into a pH 2 buffer over the concentration range of 0.1 µM–10.0 µM are illustrated in Fig. 8. Additions of pindolol result in an increase in the current intensity of the respective oxidation peak and a small displacement of potential into anodic regions. The inserted graph (Fig. 8A) shows the linear calibration curve obtained from the voltammograms. A total of three consecutive measurements ($N$ = 3) were used to construct a calibration curve over the linear range 0.1–10.0 µM with a limit of detection (3σ) found to be 0.097 µM (for more information and a summary, see Table 1). Whilst the limit of detection using SPEs is comparable with the previously reported method using RGO modified GC electrodes[15] (0.026 µM using RGO modified GC *versus* 0.097 µM for GSPEs (in this work)), the SPEs are preferable since they do not require a pre-treatment step nor require modification for an improved electroanalytical response.

Table 1 The main electroanalytical parameters obtained from the calibration curve for pindolol detection in 0.1 M KCl supporting electrolyte utilizing square wave voltammetry and SPEs

| | |
|---|---|
| Linear concentration range (µmol $L^{-1}$) | 0.1–10.0 |
| Slope of calibration graph (A L $mol^{-1}$) | 0.091 |
| Intercept (A) | 0.0291 |
| Correlation coefficient | 0.9996 |
| Relative standard deviation (%RSD) | 2.19 |
| LOD (µmol $L^{-1}$) | 0.097 |
| LOQ (µmol $L^{-1}$) | 0.322 |

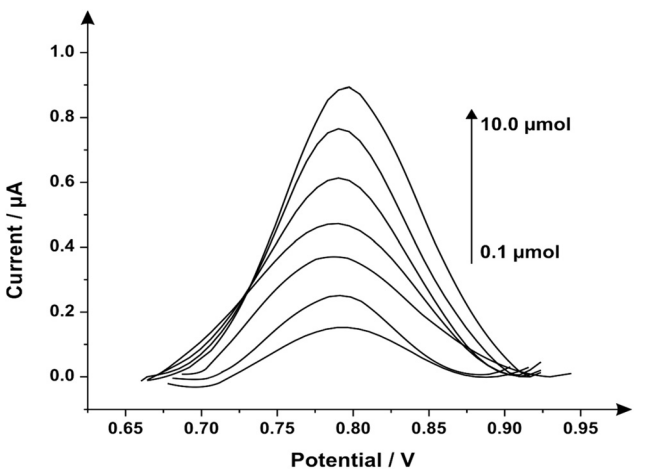


Fig. 9 Square wave voltammograms recorded over a range of pindolol concentrations (0.1–10 µM) in a urine sample using the standard addition method (step potential = 0.00705 V, frequency = 50 Hz, amplitude = 50 mV, deposition potential = 0.5 V and duration = 10 s *vs.* Ag/AgCl) and SPEs.

### Analysis of real samples

To verify the applicability and resourcefulness of the standard addition method, human urine samples were analyzed using

Table 2 Recovery of pindolol from human urine samples at various concentrations

| Concentration aliquots [μM] | Concentration found [μM] | Recovery [%] |
|---|---|---|
| 0.1 | 0.185 | 185.0 |
| 0.3 | 0.390 | 130.0 |
| 0.5 | 0.582 | 116.4 |
| 0.7 | 0.778 | 111.1 |
| 1.0 | 1.135 | 113.5 |
| 2.0 | 2.310 | 115.5 |
| 10.0 | 10.80 | 108.0 |
| 13.0 | 13.30 | 102.3 |
| 15.0 | 15.50 | 103.3 |
| 17.0 | 17.00 | 100.0 |
| 20.0 | 21.10 | 105.5 |

the same parameters (for square wave) as those described above, see Fig. 9 for a representative example. Human urine is composed of various substances, such as uric acids, salts and nitrogenous products of metabolism (interferents),[43,44] so dilution of the sample is required in order to obtain an optimal electrochemical response (see the Experimental section). The method proved to be highly sensitive for detecting low concentrations of our target analyte. In light of these results, the proposed analytical protocol can be successfully and easily used in the evaluation and recovery of pindolol from human urine (Table 2).

## Conclusions

We have demonstrated the potential utilization of screen-printed graphite electrodes for the determination of pindolol. These screen-printed graphite electrodes allow the rapid and facile determination of the β-blocker without recourse to pre-treatment or pre-concentration, resulting in an improved response in comparison to alternative electrode materials, such as boron-doped diamond and glassy carbon. It was found that improvements in the electroanalytical performance of the screen-printed configuration could not be yielded through modification with reduced graphene oxide, as has previously been reported.[15] When considering the electroanalytical performance of the screen-printed graphite electrodes it was evident that enhanced sensitivity and limits of detection were facilitated through incorporation of square wave voltammetric techniques. Furthermore, this low cost, highly reproducible and reliable sensor was demonstrated to offer an excellent determination of pindolol in traditionally troublesome samples, such as urine. The bare (unmodified) SPE sensing platforms are comparable (analytically) to prior reports using RGO modified glassy carbon electrodes[15] and do not require any electrode modification (*i.e.* polishing or modification with RGO) or pre-treatment, and hence we question the need to use RGO in the first place. In comparison of our work against prior analytical (non-electrochemical technologies), the analytical performance of our electroanalytical protocol can be considered superior to that previously reported research[45–49] because of the inessential pre-treatment and modification of the surface whilst also being cheap and disposable sensors.

## Acknowledgements

Financial support for this research was supplied by Co-ordenação de Aperfeiçoamento de Pessoal de Nível Superior (CAPES).

## References

1 K. Kim, E. Cho, J. M. Choi, H. Kim, A. Jang, Y. Choi, I. S. Lee, J.-H. Yu and S. Jung, *Carbohydr. Polym.*, 2014, **106**, 101–108.
2 R. A. E. Castro, J. Canotilho, S. C. C. Nunes, M. E. S. Eusébio and J. S. Redinha, *Spectrochim. Acta, Part A*, 2009, **72**, 819–826.
3 A. Motoyama, A. Suzuki, O. Shirota and R. Namba, *J. Pharm. Biomed. Anal.*, 2002, **28**, 97–106.
4 A. B. Jeppsson, U. Johansson and B. Waldeck, *Acta Pharm. Toxicol.*, 1984, **54**, 285–291.
5 S. C. C. Nunes, M. E. Eusébio, M. L. P. Leitão and J. S. Redinha, *Int. J. Pharm.*, 2004, **285**, 13–21.
6 A. Ellenbogen, O. Jaschevatzky, A. Davidson, S. Anderman and S. Grunstein, *Int. J. Gynecol. Obstet.*, 1986, **24**, 3–7.
7 D. Martinez, A. Broft and M. Laruelle, *Biol. Psychiatry*, 2000, **48**, 844–853.
8 G. L. Perlovich, T. V. Volkova and A. Bauer-Brandl, *Mol. Pharm.*, 2007, **4**, 929–935.
9 J. Ballesteros and L. F. Callado, *J. Affective Disord.*, 2004, **79**, 137–147.
10 C. Gazpio, M. Sánchez, A. Zornoza, C. Martín, C. Martínez-Ohárriz and I. Vélaz, *Talanta*, 2003, **60**, 477–482.
11 A. A. Salem, I. A. Wasfi and S. S. Al-Nassibi, *J. Chromatogr., B: Biomed. Appl.*, 2012, **908**, 27–38.
12 S. K. T. Chelvi, J. Zhao, L. Chen, S. Yan, X. Yin, J. Sun, E. L. Yong, Q. Wei and Y. Gong, *J. Chromatogr., A*, 2014, **1324**, 104–108.
13 J. L. Beal and S. E. Tett, *J. Chromatogr., B: Biomed. Appl.*, 1998, **715**, 409–415.
14 C. Gazpio, M. Sánchez, I. X. García-Zubiri, I. Vélaz, C. Martínez-Ohárriz, C. Martín and A. Zornoza, *J. Pharm. Biomed. Anal.*, 2005, **37**, 487–492.
15 S. Smarzewska and W. Ciesielski, *Anal. Methods*, 2014, **6**, 5038–5046.
16 E. P. Randviir, D. A. C. Brownson, J. P. Metters, R. O. Kadara and C. E. Banks, *Phys. Chem. Chem. Phys.*, 2014, **16**, 4598–4611.
17 J. P. Metters, D. K. Kampouris and C. E. Banks, *Analyst*, 2014, **139**, 3999–4004.
18 C. W. Foster, J. P. Mettters, D. K. Kampouris and C. E. Banks, *Electroanalysis*, 2014, **26**, 262.

19 J. P. Smith, J. P. Metters, D. K. Kampouris, C. Lledo-Fernandez, O. B. Sutcliffe and C. E. Banks, *Analyst*, 2013, **138**, 6185.
20 A. V. Kolliopoulos, J. P. Metters and C. E. Banks, *Anal. Methods*, 2013, **5**, 3490–3496.
21 J. Metters, F. Tan and C. Banks, *J. Solid State Electrochem.*, 2013, **17**, 1553–1562.
22 F. Tan, J. P. Metters and C. E. Banks, *Sens. Actuators, B*, 2013, **181**, 454–462.
23 O. Ramdani, J. P. Metters, L. C. S. Figueiredo-Filho, O. Fatibello-Filho and C. E. Banks, *Analyst*, 2013, **153**, 1053.
24 J. P. Smith, J. P. Metters, C. Irving, O. B. Sutcliffe and C. E. Banks, *Analyst*, 2014, **139**, 389–400.
25 J. P. Metters, R. O. Kadara and C. E. Banks, *Analyst*, 2011, **136**, 1067–1076.
26 M. Gómez-Mingot, J. Iniesta, V. Montiel, R. O. Kadara and C. E. Banks, *Sens. Actuators, B*, 2011, **155**, 831–836.
27 B. Yu, D. Kuang, S. Liu, C. Liu and T. Zhang, *Sens. Actuators. B*, 2014, **205**, 120–126.
28 D. A. C. Brownson, S. A. Varey, F. Hussain, S. J. Haigh and C. E. Banks, *Nanoscale*, 2014, **6**, 1607–1621.
29 D. Graf, F. Molitor, K. Ensslin, C. Stampfer, A. Jungen, C. Hierold and L. Wirtz, *Nano Lett.*, 2007, **7**, 238–242.
30 L. C. S. Figueiredo-Filho, D. A. C. Brownson, M. Gomez-Mingot, J. Iniesta, O. Fatibello-Filho and C. E. Banks, *Analyst*, 2013, **138**, 6354–6364.
31 D. A. Brownson, D. K. Kampouris and C. E. Banks, *Chem. Soc. Rev.*, 2012, **41**, 6944–6976.
32 K. N. Kudin, B. Ozbas, H. C. Schniepp, R. K. Prud'homme, I. A. Aksay and R. Car, *Nano Lett.*, 2007, **8**, 36–41.
33 G. K. Ramesha and S. Sampath, *J. Phys. Chem. C*, 2009, **113**, 7985–7989.
34 H. Park, H. Ahn, Y. Chung, S. Baek Cho, Y. Soo Yoon and D.-J. Kim, *Mater. Lett.*, 2014, **136**, 164–167.
35 P. F. Li, Y. Xu and X.-H. Cheng, *Surf. Coat. Technol.*, 2013, **232**, 331–339.
36 P. F. Li, H. Zhou and X. Cheng, *Surf. Coat. Technol.*, 2014, **254**, 298–304.
37 A. J. Bard and L. R. Faulkner, *Electrochemical Methods: Fundamentals and Applications*, Wiley, 2000.
38 B. de Castro, V. Domingues, P. Gameiro, J. L. F. C. Lima, A. Oliveira and S. Reis, *Int. J. Pharm.*, 1999, **187**, 67–75.
39 M. Amouzadeh Tabrizi and J. N. Varkani, *Sens. Actuators, B*, 2014, **202**, 475–482.
40 J.-X. Feng, Q.-L. Zhang, A.-J. Wang, J. Wei, J.-R. Chen and J.-J. Feng, *Electrochim. Acta*, 2014, **142**, 343–350.
41 D. A. C. Brownson, A. C. Lacombe, M. Gomez-Mingot and C. E. Banks, *RSC Adv.*, 2012, **2**, 665–668.
42 L. C. S. Figueiredo-Filho, D. A. C. Brownson, O. Fatibello-Filho and C. E. Banks, *Analyst*, 2013, **138**, 4436–4442.
43 W. Guan, X. Duan and M. A. Reed, *Biosens. Bioelectron.*, 2014, **51**, 225–231.
44 H. Dubois, B. Delvoux, V. Ehrhardt and H. Greiling, *J. Clin. Chem. Clin. Biochem. Z. Klin. Chem. Klin. Biochem.*, 1989, **27**, 151–156.
45 D. Pecanac, D. Radulovic, L. Zivanovic and S. Agatonovic-Kustrin, *J. Pharm. Biomed. Anal.*, 1991, **9**, 861–864.
46 T. Perez Ruiz, C. Martinez-Lozano, V. Tomas and J. Carpena, *Talanta*, 1998, **45**, 969–976.
47 R. A. S. Lapa, J. Lima, B. F. Reis, J. L. M. Santos and E. A. G. Zagatto, *Anal. Chim. Acta*, 1998, **366**, 209–215.
48 S. Khalil and N. Borham, *J. Pharm. Biomed. Anal.*, 2000, **22**, 235–240.
49 S. Khalil and M. M. El-Rabiehi, *J. Pharm. Biomed. Anal.*, 2000, **22**, 7–12.